Liquid/Liquid Interface Polymerized Porphyrin Membranes Displaying Size-Selective Molecular and Ionic Permeability

Jodi L. O'Donnell, Numrin Thaitrong, Andrew P. Nelson, and Joseph T. Hupp*

Department of Chemistry, Northwestern University, Evanston, Illinois 60208-3113

Thin polymeric membranes have been formed by liquid/liquid interfacial copolymerization of a sterically demanding tetraphenylporphyrin derivative having reactive phenol substituents and a second porphyrin having reactive acid chloride groups. The out-of-plane steric demand is created by 3,5-hexoxyphenyl groups positioned at two of the four meso carbons of the porphyrin ring. The bulky substituents were designed to create local pockets and extended pores within the resulting ester-linked copolymer. Quantitative measures of molecular and ionic transport were obtained by placing membranes over microelectrodes and recording voltammetric responses from redox-active probes. The membranes were found to be permeable to small molecules and ions, but blocking toward larger ones, displaying a sharp size cutoff at a probe diameter of ca. 3.5 Å. Molecular transport can be modulated by axially ligating pore-blocking moieties to available porphyrin metal centers.

Introduction

The ability of porphyrins to stabilize coordinatively unsaturated metal ions has rendered them molecules of choice for an enormous number of investigations of chemical catalysis, electrocatalysis, and chemical sensing. Their structural and functional similarity to chlorophyll has made them the focus of a similarly vast number of studies of photophysical and photochemical processes, including solar-cell-related processes. In many cases, the functional properties of porphyrinic molecules are best exploited by organizing them as thin films on solid support structures.[1−4] If such films could be prepared without the assistance of solid supports and if they could be fashioned with molecular-scale permeability, other interesting applications could be envisioned including ones involving membrane catalysis, chemically selective transport, and/or molecular sieving.

Recently, we reported on the synthesis and molecular-transport properties of apparently the first such porphyrin films or membranes of this kind.[5,6] The membranes were formed by polymerization of a hollow molecule, the tetra-porphyrinic square assembly **1**, at the interface of an immiscible pair of liquids (water and dichloromethane). Liquid/liquid interfacial polymerization is attractive for membrane fabrication because it is self-healing, at least during the growth phase, and self-limiting, allowing pinhole-free films of controllable thickness to be obtained.[7] The polymerization of **1** was accomplished by condensation of porphyrin-pendant phenol functionalities (water phase) with acid chloride termini of short alkyl cross-linkers

(nonaqueous phase). The resulting membranes were found to be highly permeable to small and medium-sized molecules, but completely blocking toward large molecules. Notably, the observed sharp molecular size cutoff coincided with the modeled size of the cavity defined by an isolated square assembly, ca. 24 Å.
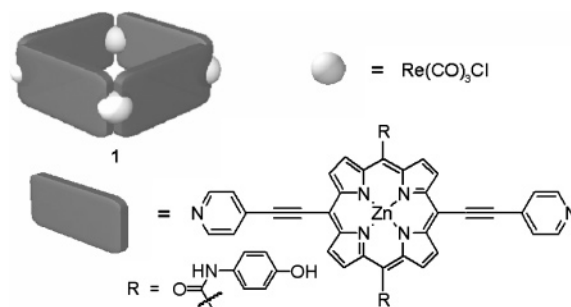
We now report the synthesis of a porphyrin-based membrane material displaying much finer molecular sieving. In place of a molecular square or other hollow building block, we have taken a simpler approach and used a highly sterically encumbered monomeric porphyrin, **5**. Wamser and co-workers have previously shown that robust nonporous polymeric films can be obtained via interfacial condensation of unencumbered porphyrins.[7−9] By cross-linking **5** with a conventionally shaped porphyrin, we obtain polymeric membranes containing extended pores having minimum diameters of about 3.5 Å. We find that the membranes are readily permeated by molecules and ions having diameters of less than ∼3.5 Å, but are essentially blocking toward larger candidate permeants, i.e., a sharp molecular size cutoff is found.

* Corresponding author. E-mail: jthupp@chem.northwestern.edu.

(1) Suslick, K. S.; Rakow, N. A.; Sen, A. *Langmuir* **2004**, *60*, 11133−11138.

(2) Splan, K. E.; Hupp, J. T. *Langmuir* **2004**, *20*, 10560−10566.

(3) Hasobe, T.; Imahori, H.; Fukuzumi, S.; Kamat, P. V. *J. Phys. Chem. B* **2003**, *107*, 12105−12112.

(4) Benitez, I. O.; Bujoli, B.; Camus, L. J.; Lee, C. M.; Odobel, F.; Talham, D. R. *J. Am. Chem. Soc.* **2002**, *124*, 4363−4370.

(5) Keefe, M. H.; O'Donnell, J. L.; Bailey, R. C.; Nguyen, S. T.; Hupp, J. T. *Adv. Mater.* **2003**, *15*, 1936−1939.

(6) Murray and co-workers have reported on the synthesis and molecular permeability of electrode-supported films obtained via oxidative electropoly-merization of tetra(*ortho*-aminophenyl)porphyrin species. See, for example: Pressprich, K. A.; Maybury, S. G.; Thomas, R. E.; Linton, R. W.; Irene, E. A.; Murray, R. W. *J. Phys. Chem.* **1989**, *93*, 5568−5574. Also see: Malinski, T.; Ciszewski, A.; Fish, J. R. *Anal. Chem.* **1990**, *62*, 909−914.

(7) Wamser, C. C.; Bard, R. R.; Senthilathipan, V.; Anderson, V. C.; Yates, J. A.; Lonsdale, H. K.; Rayfield, G. W.; Friesen, D. T.; Lorenz, D. A. *J. Am. Chem. Soc.* **1989**, *111*, 8485−8491.

(8) Li, W.; Wamser, C. C. *Langmuir* **1995**, *11*, 4061−4071.

(9) Wamser and co-workers suggest, on the basis of cell resistance measurements, that the films described in ref 8 are permeable to electrolyte solutions. Using the electrochemical methodology described below, however, we find these films to be completely blocking toward the smallest redox probe salt examined, sodium iodide. Nevertheless, under certain conditions, with thinner films than described here, we do observe electrochemical responses from probe ions and molecules. The responses are both large and insensitive to probe size, indicating that probes reach the electrode by passing through film physical defects (probably tears), rather than by permeating the film material itself. We suggest that physical defects similarly might well account for the reported low cell resistances.

Scheme 1. Synthesis of Porphyrin 5
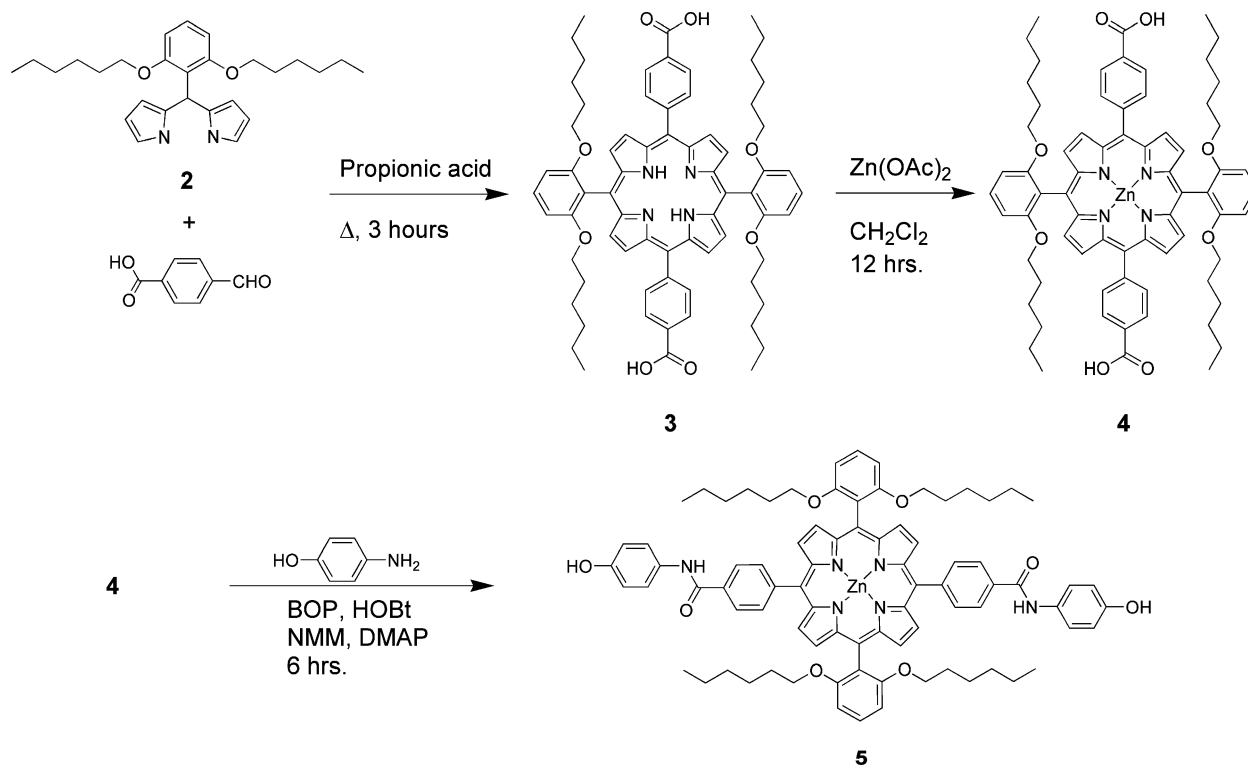
We additionally find that transport can be modulated by axially ligating pore-blocking moieties to available porphyrin metal centers.

Experimental Methods

Materials. All reagents were used as received unless otherwise specified.

Synthesis. A summary of synthetic conditions can be found in Scheme 1.

Meso-[2,6-di(*n*-hexoxy)phenyl]dipyrromethane(2)[2] and Tetrakis[4-(chlorocarbonyl)phenyl]porphyrin(6).[7] These materials were synthesized as described previously. The purity of **6** was verified by high-resolution FAB-MS 865.07 (MH+ *m/z* calculated), 865.1 (observed).

5,15-Bis[4-carboxyphenyl]-10,20-bis[2,6-di(*n*-hexoxy)phenyl]-porphyrin (3). Meso-(2,6-dihexoxyphenyl)dipyrromethane (**2**; 423 mg, 1 mmol) and 4-carboxybenzaldehyde (178 mg, 1 mmol) were combined under N$_2$ in 8 mL of propionic acid. The reaction mixture was refluxed under a stream of N$_2$ for 3 h. The propionic acid was removed in vacuo, and the resulting mixture was dissolved in methylene chloride. The solution was neutralized by washing three times with saturated potassium carbonate solution and then dried over magnesium sulfate. Solvent was removed by rotary evaporation. The desired product was isolated as the second of two porphyrin products via column chromatography (silica, 8:1:0.01 hexanes/ethyl acetate followed by acetone) to yield a purple solid (130 mg, 22%). ^{1}H NMR (400 MHz, CDCl$_3$) 8.84 (d, 4H, *J* = 4.88 Hz), 8.72 (d, 4H, *J* = 3.66 Hz), 8.49 (d, 4H, *J* = 7.32 Hz), 8.32 (d, 4H, *J* = 7.32 Hz), 7.69 (t, 2H, *J* = 8.55 Hz), 6.98 (d, 4H, *J* = 8.55 Hz), 3.83 (t, 8H, *J* = 6.10 Hz), 0.941 (q, 8H *J* = 6.01 Hz), 0.53 (m, 16H), 0.40 (m, 8H), 0.41 (q, 8H *J* = 6.10 Hz), 0.26 (t, 12H *J* = 6.10 Hz) −2.64 (s, 2H). MALDI-MS 1104.39 (MH+, *m/z* calculated), 1105.32 (observed).

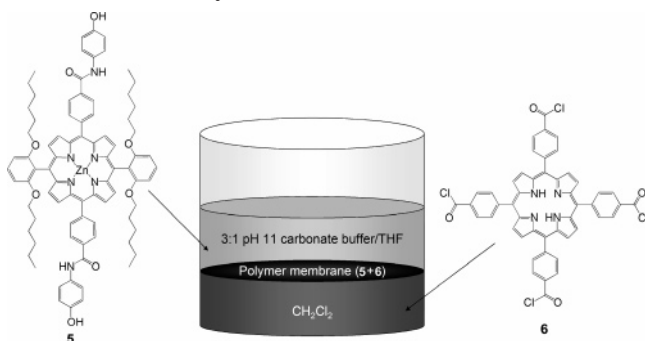**[5,15-Bis(4-carboxyphenyl)-10,20-bis(2,6-dihexoxyphenyl)por-phinato]zinc(II) (4).** Zinc acetate (50 mg, 0.27 mmol, dissolved in 5 mL of methanol) and **3** (30 mg, 0.026 mmol) were added to methylene chloride and stirred in the dark under N$_2$ overnight. The reaction mixture was washed with brine to remove excess zinc acetate and acetic acid, dried over magnesium sulfate, and dried under reduced

pressure to yield a purple solid (30 mg, 95%). ^{1}H NMR (500 MHz, CDCl$_3$) 8.92 (d, 4H, *J* = 4.28 Hz), 8.80 (d, 4H, *J* = 4.28 Hz), 8.46 (d, 4H, *J* = 7.33 Hz), 8.31 (d, 4H, *J* = 7.94 Hz), 7.69 (t, 2H, *J* = 8.55 Hz), 7.11 (d, 4H, *J* = 7.94 Hz), 6.99 (d, 4H, *J* = 8.55 Hz), 6.79 (d, 4H, *J* = 8.55), 3.84 (q, 4H, *J* = 6.11 Hz), 0.88 (m, 14H), 0.84 (m, 16H), 0.48 (m, 8H), 0.330 (q, 8H), 0.20 (t, 12H, *J* = 7.33 Hz) ppm. MALDI-MS 1167.8 (MH+, *m/z* calculated) 1167.2 (observed).

[5,15-bis(*N*-4-hydroxy)benzamidylphenyl]-10,20-bis[2,6-(di-hexoxyphenyl)porphinato]Zn(II) (5). Zinc porphyrin **4** (16 mg, 0.014 mmol) was dissolved in 10 mL of dry tetrahydrofuran. Standard peptide coupling reagents[10] *n*-methylmorpholine (NMM) (14 µL, 0.125 mmol), benzotriazol-1-yloxytris(dimethylamino)phosphonium hexafluorophosphate (BOP) (53 mg, 0.125 mmol), 1-hydroxyben-zotriazole (HOBt) (17 mg, 0.25 mmol), and (dimethylamino)pyridine (DMAP) (12 mg, 0.098 mmol) were added, and the mixture was stirred in air for 15 min.[10] 4-Aminophenol (26 mg, 0.24 mmol) was added, and the reaction mixture was stirred in the dark for 6 h. The resulting solution was filtered through a Celite plug, and the solvent was removed by rotary evaporation. The solid was redissolved in methylene chloride, washed with brine, and dried over calcium chloride, and the solvent was removed by rotary evacuation. The product was isolated via column chromatography (silica, 98:2 methylene chloride/methanol) yielding a maroon powder (22 mg, 38%). ^{1}H NMR (500 MHz CDCl$_3$) 8.89 (d, 4H, *J* = 4.0 Hz), 8.83 (d, 4H, *J* = 4.8 Hz) 8.33 (d, 4H, *J* = 8.0 Hz), 8.22 (d, 4H, *J* = 7.6 Hz), 7.70 (t, 2H, *J* = 8.2 Hz), 7.01 (d, 4H, *J* = 8.8 Hz), 6.92 (m, 8H), 3.86 (t, 8H, *J* = 5.6 Hz), 0.91 (m, 8H), 0.51 (m, 16H), 0.33 (m, 8H), 0.25 (m, 12H). FAB-MS (high-resolution) 1347.58 (MH+, *m/z* calculated) 1347.2 (observed).

Membranes. Polymeric membranes were prepared and characterized in a manner similar to that used in previous work.[5] The general procedure for the interfacial polymerization as depicted in Scheme 2 was as follows: The phenolic zinc porphyrin **5** (1.0 mg, 0.74 µmol) was dissolved in 250 µL of tetrahydrofuran. Then, 750 µL of pH 11 aqueous buffer was added to make 1 mL of solution. This mixture was layered over 2 mL of a 3 mM solution of **6** in methylene chloride in a 10-mL beaker. A circular glass disk with a diameter matching the inner dimensions of the 10-mL beaker

(10) Hudson, D. *J. Org. Chem.* **1988**, *53*, 617−624.

Scheme 2. Interfacial Polymerization of 5 and 6 to Form Polymer Membrane (5 + 6)

Figure 1. Molecular model of **5** showing its 3-D structure (Hyperchem 6.02).

fitted with a glass rod attached at a 90° angle to the base was placed inside the beaker prior to the addition of reagents. Following the addition of reagents, the beaker was placed in a sealed jar overnight. The membrane was then removed from the beaker by slowly removing the circular disk to which the membrane temporarily adheres and transferred to a THF reservoir to rinse unreacted monomers from the film surface. The membrane was then either immediately deposited on an electrode or stored in water for future use. Deposition was done by removing a small piece of film from the liquid reservoir with a spatula and then forcing it onto the substrate with a stream of acetone from a microliter syringe. Membranes that had been stored in water tended to crack following removal, deposition, and drying on an electrode surface, presumably because of changes in capillary forces during water evaporation. Cracking was avoided by rinsing the membranes with acetone or another low-viscosity solvent before deposition.

Measurements. Electronic absorption spectra were recorded on a Varian Cary 5000 UV−vis−NIR spectrophotometer after membrane deposition on glass slides. Membrane thicknesses were measured by profilometry (Tencor P-10 profilometer) or atomic force microscopy (Bioscope AFM, Digital Instruments).

Electrochemical data were obtained with a CH Instruments (Austin, TX) model 900 bipotentiostat. All voltammetry measurements were performed in aqueous solution using a Pt counter electrode, a Ag/AgCl reference electrode, and one or two 10-μm Pt working electrode(s) (CH Instruments). At the sweep rates used (10−30 mV/s), the electrode shows a quasi-steady-state sigmoidal, rather than peaked, voltammetric response. The membrane orientation over the electrode was observed visually with a CCD camera (Panasonic KR222, Edmund Scientific) and a video monitor. Purified 18-MΩ water (Millipore) was used to prepare 1−3 mM permeant solutions with either 0.1 or 0.2 M supporting electrolyte. A few measurements (noted below) were done in acetonitrile as the solvent.

Results and Discussion

Synthesis and Interfacial Polymerization of 5. The synthesis of **5** is shown in Scheme 1. The starting porphyrin, **3**, was synthesized by a modified version of MacDonald [2 + 2] condensation.[11,12] Exposure to Zn(OAc)$_2$ resulted in metalation of the porphyrin. The resulting carboxylic acid substituents were coupled to 1,4-aminophenol in the presence of standard peptide coupling reagents.[10] Shown in Figure 1 is a stick model of **5** that illustrates the 3-D nature of this porphryin's structure. From the structure, we anticipated that the bulky phenyl ether substituents, orthogonally oriented to the tetrapyrrole plane, might define useable cavities and pores in subsequently prepared polymers.

A variety of candidate cross-linkers were scouted in test polymerizations done with commercially available or more readily synthesized hydroxyl- or amine-terminated porphyrins. Included among the evaluated cross-linkers were succinyl chloride, adipoyl
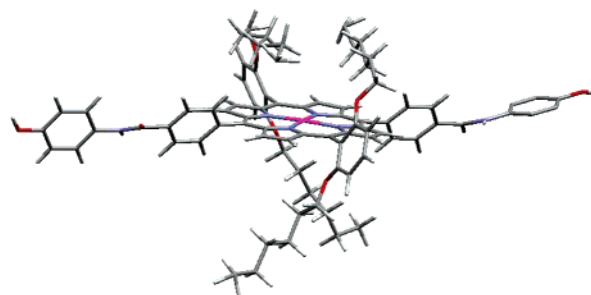
chloride, sebacoyl chloride, and tetrakis[4-(chlorocarbonyl)-phenyl]porphyrin (**6**) (Table 1). Porphyrin **6** was identified as the best cross-linker for making polymer films exhibiting sufficient mechanical stability for subsequent manipulation. The final membrane polymerization scheme is illustrated in Scheme 2.

Figure 2 shows a representative visible-region absorption spectrum for the copolymer of **5** and **6**. Also shown are spectra for the unreacted monomers. Monomer **6** displays the pattern of four low-energy Q-bands expected for a free-base porphyrin, whereas **5** displays only two Q-bands, as expected for a metalated porphyrin. Although spectral broadening accompanies polymerization, Q-bands characteristic of the monomers are clearly discernible for the polymer.

Although we have described the formation of films of (**5** + **6**) as similar to the formation of films from hollow molecular squares, there are important differences. Square films remain permeable to the small co-reactant used. Consequently, film growth can continue even after a continuous membrane is formed. Polymerization of **5** and **6**, however, produces a material that is blocking toward both reactants. Film growth at later stages must be occurring by reactant transport through physical defects. Once all of these are filled, growth stops. It follows that films grown to less than maximum thickness will contain pinholes or other defects.

Electrochemical Assessment of Membrane Permeability and Sieving Behavior. Membranes were placed over 10-μm-diameter platinum microelectrodes. Film orientation and continuity were evaluated visually with a CCD camera (Panasonic KR222, Edmund Scientific). Membrane permeability with respect to a series of redox-active probe molecules was evaluated using slow-sweep (quasi-steady-state, 10−30 mV/s) cyclic voltammetry. These measurements take advantage of two useful features of electrochemical measurements. First, because current is a measure of molecular flux, rates of transport are proportional to the amount of current observed for a given reduction−oxidation cycle. Second, reduction or oxidation of a probe molecule at an electrode can occur only if both the anion and cation can reach the working electrode, which is placed beneath the membrane. If the membrane prevents transport of the probe species to the electrode, no current will be observed, giving a measure of the size of the pores of the membrane based on the size of the probes.
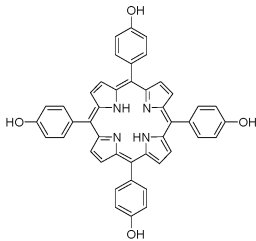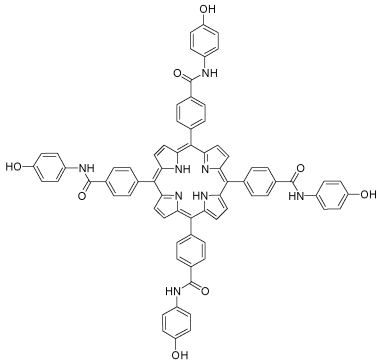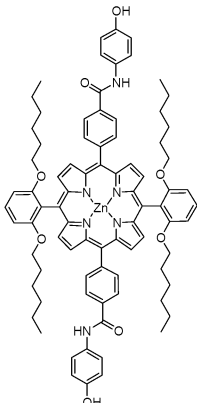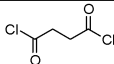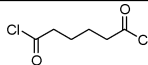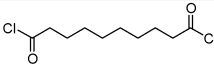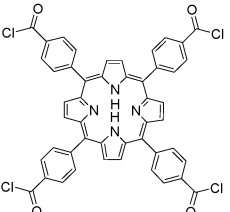
Preliminary experiments with redox-active probes that we have used previously (for example, with polymeric films derived from **1**) showed that all were blocked. The smallest probe, ferrocenemethanol, has a radius of about 3.6 Å.[13] When smaller probe species were evaluated, it was found that iodide and nitrobenzene (r = 2.1 and ∼3.1 Å respectively) were able to traverse the

(11) Arsenault, G. P.; Bullock, E.; MacDonald, S. F. *J. Am. Chem. Soc.* **1960**, *82*, 4384−4389.

(12) MacDonald, S. F. *J. Am. Chem. Soc.* **1957**, *79*, 2659.

(13) This value represents measured distances between Fe and the center of a cyclopentadienyl (cp) ring from structures in the Cambridge Database plus one van der Waals carbon radius. The actual radius could be slightly larger depending on the orientation of methanol substituent.

Table 1. Film Thicknesses as a Function of Crosslinker Identity

	(THPP)[a]	(THACPP)[b]	(5)[c]
Cross linker *(chain length[d])*	*Film Thickness[e](nm)*	*Film Thickness (nm)*	*Film Thickness (nm)*
Succinyl chloride (3.8 Å)	400 ± 150	N/A	N/A
Adipoyl chloride (6.4 Å)	760 ± 420	170 ± 50	N/A
Sebacoyl chloride (11.5 Å)	830 ± 300	500 ± 330	N/A
TClCPP (6) (17.9 Å)	3800 ± 900	500 ± 160	960 ± 160

[a] 1.5 mM THPP in THF/buffer pH 11 and 1.2 mM cross linkers in CH_2Cl_2, 24 h. [b] 0.9 mM THACPP in THF/buffer pH 11 and 1.2 mM cross linkers in CH_2Cl_2, 17 h. [c] 1.5 mM porphyrin 6 in THF/buffer pH 11 and 1.2 mM cross linkers in CH_2Cl_2, 16 h. [d] Distance between carbonyl carbons as estimated by molecular mechanics using Hyperchem 6.02. [e] All film thicknesses measured by profilometry.

membrane. Figure 3a shows the electrochemical response associated with transport of sodium iodide through a film, and Figure 3b demonstrates the blocking of ferrocenemethanol by the same membrane. The observation of blocking behavior is important because it serves to establish that the current seen with smaller probes is indeed due to membrane permeation, rather than pinhole transport.

Returning to Figure 3a, the observed attenuation of the current for iodide oxidation current is a consequence of slower transport through the film than through the external solution. Film transport could be limited by either slow solution-to-film partitioning kinetics or slow diffusion within the film. In principle, the two can be distinguished by making measurements as a function of membrane thickness, d. Unfortunately, only the thickest films are pinhole-free, a not unexpected result.

If we assume, on the basis of experience with other systems, that transport is limited by film diffusion, then currents (i.e.,

permeant fluxes) measured in the plateau region of steady-state voltammograms will be associated with well-defined film-phase concentration gradients. This circumstance allows film permeabilties to be estimated. The permeability is defined as the product of the permeant's solution-to-film partition coefficient, P, and its diffusion coefficient in the film phase, D_f. The relation between the permeability and the observed plateau current, i_{film}, is

$$\frac{i}{i_{film}} = 1 + \frac{4D_s d}{\pi r P D_f} \qquad (1)$$

where i is the observed current for a bare electrode, i_{film} is the observed current for a film modified electrode, D_s is the probe molecule's diffusion coefficient in solution, d is the film thickness, r is the microelectrode radius, P is the solution-to-membrane partition coefficient, and D_f is the diffusion coefficient within the membrane.[5]
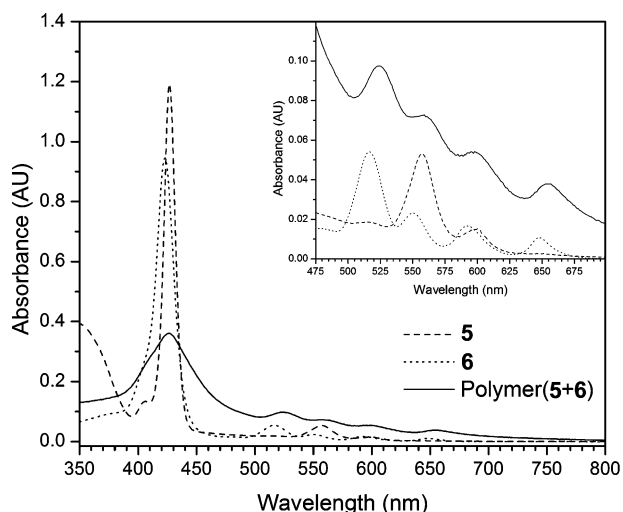
Figure 2. Electronic absorption spectra of **5**, **6**, and polymer (**5** + **6**). Inset: Zoom view of absorbance in the porphyrin Q-band region.
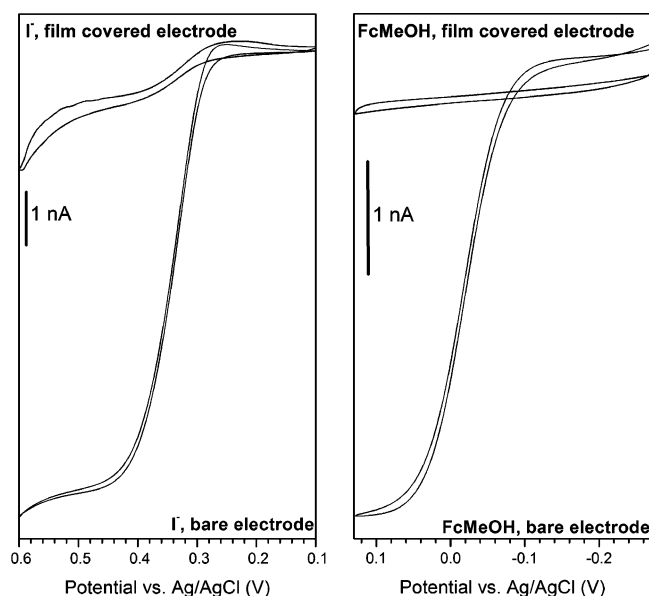
Figure 3. Steady-state cyclic voltammograms of sodium iodide and ferrocenemethanol probes on bare and polymer-covered microelectrodes, Scan rate, 30 mV/s, NaI probe solution concentration, 2 mM with 200 mM aqueous $NaNO_3$ as the supporting electrolyte; FcMeOH probe solution, 3 mM with 100 mM aqueous $NaNO_3$ as the supporting electrolyte.

Quantitative voltammetry experiments with profilometry-measured films of thickness 970 ± 160 nm yielded a PD_f value of $\sim 6 \times 10^{-7}$ cm²/s for sodium iodide. (In applying eq 1, we have implicitly assumed that the film thickness is reasonably uniform. If instead many thin spots exist, the true permeability will be smaller.) For similarly fabricated porous membranes composed of porphyrinic molecular square subunits, the permeation rate would be at least quadruple this value according to extrapolation of data from larger probes,[5] indirectly suggesting that the pore dimensions of these membranes examined here are subnanometer. For comparison, the microelectrode-measured diffusion coefficient for I^- in solution, with Na^+ as the counterion, is 200×10^{-7} cm²/s.

Quantitative Evaluation of Molecular Sieving. To obtain a more quantitative estimate of pore of size, we chose to examine I^- oxidation while systematically changing the size of the cation that accompanies the iodide anion through the film.[14] The permeant cations evaluated were Na^+, NH_4^+, NMe_4^+, NEt_4^+,
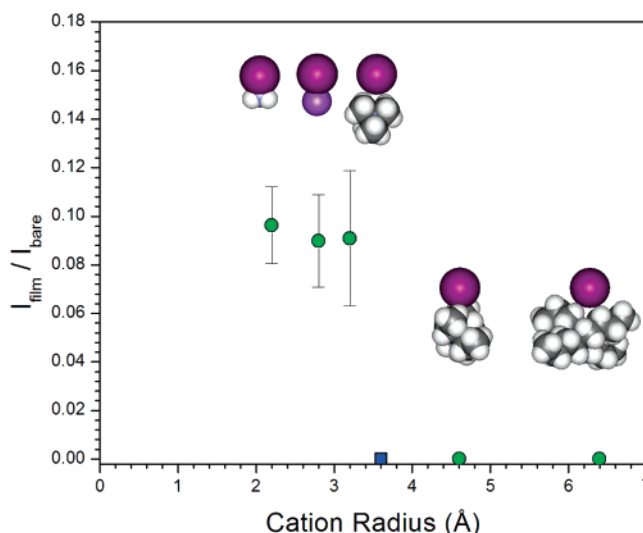
Figure 4. Plot of i_{film}/i_{bare} [with and without polymer (**5** + **6**)] ratio of steady-state currents measured at a 10-μm Pt working electrode as a function of cation radius for the iodide salts of NH_4^+, Na^+, $N(CH_3)_4^+$, $N(C_2H_5)_4^+$, and $N(C_4H_9)_4^+$. Film thicknesses were 960 nm. The lone square point corresponds to ferrocenemethanol (structure not shown).

and NBu_4^+ [radii (r) = 2.8 (hydrated radius), 2.2, 3.2, 4.6, and 6.4 Å, respectively). In each measurement, the electrolyte was the nitrate salt of the chosen cation. This ensured that no smaller counterions were present to facilitate the transport of I^- through the film. The iodide salt concentration was 2 mM. The concentration of the redox-inert electrolyte was 200 mM. The measurements were made using a four-electrode setup featuring two working electrodes: one with a film on its surface and one bare electrode such that the ratio of current through a membrane-covered electrode versus a bare electrode could be determined. The two electrodes used were tested with a solution of known concentration while both were bare to ensure that the electrode radii were the same.

As shown in Figure 4, the currents measured for the three smallest cations with polymer-covered electrodes were equivalent within experimental uncertainty. We[5,15] and others[16] have previously observed, with other porous films, progressively larger currents with smaller probes. That apparently different behavior is observed here might simply indicate that iodide rather than its counterion is the transport-rate-limiting species. Consistent with this idea, we note that iodide is larger than both Na^+ and NH_4^+ and similar in size to NMe_4^+. For iodide salts of the two largest cations, no current was seen at the membrane-modified electrode, indicating that transport of these species is blocked (see Figure 4). The observed sieving behavior implies minimum membrane pore radii of between 3.2 Å (NH_4^+) and 3.6 Å (ferrocenemethanol).

The observed sharp permeant size cutoff (Figure 4) is reminiscent of the sieving behavior of films of **1**, where the molecular-square cavity was found to define minimum polymer apertures. In contrast, molecular-square films assembled in layer-by-layer fashion using zirconium(IV)/phosphonate chemistry display a gradual cutoff,[15] as do electropolymerized porphyrin films studied by Murray and co-workers.[16] For both the layer-by-layer-assembled films and the electropolymerized films, the

(14) Bélanger, S.; Anderson, B. C.; Hupp, J. T. *Electrochem. Soc. Proc.* **1998**, *98−26*, 208−214.

(15) Massari, A. M.; Gurney, R. W.; Schwartz, C. P.; Nguyen, S. T.; Hupp, J. T. *Langmuir* **2004**, *20*, 4422−4429.

(16) Pressprich, K. A.; Maybury, S. G.; Thomas, R. E.; Linton, R. W.; Irene, E. A.; Murray, R. W. *J. Phys. Chem.* **1989**, *93*, 5568−5574.
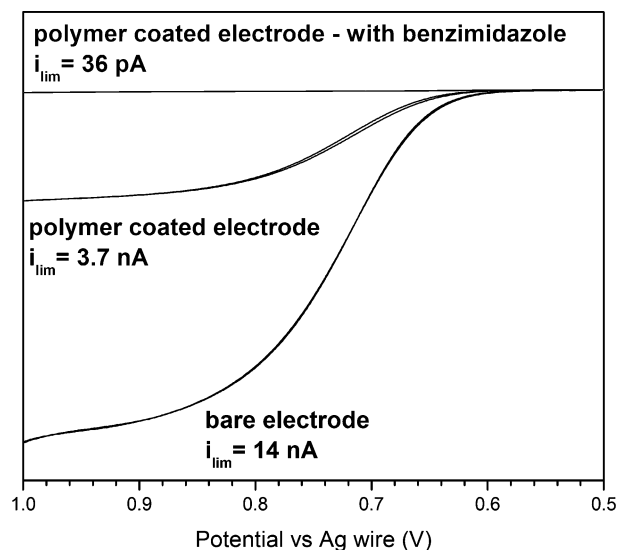
Figure 5. Blockage of transport of iodide anion through membrane by binding of benzimidazole to the zinc sites of porphyrin **5**.

gradual cutoff has been interpreted as evidence for a distribution of pore sizes.

We interpret the sharp size cutoff seen here as evidence for a more-or-less uniform minimum pore size. Our reactants differ from those of Wamser and co-workers only in that they make substantial steric demands in the direction normal to the plane of the porphyrin. This precludes tight polymer layer stacking in the sense of achieving van der Waals contact between porphyrin planes. Stacking and associated cross-linking presumably accounts for the lack of porosity of the previously studied films. The proposed internal structure of the membrane based on (**5** + **6**) is one in which there is no pore regularity or organization. Instead, tortuous paths, containing bottlenecks, are presented to permeants. We suggest that the uniformly sized bottleneck sites are the pockets created by hexoxyphenyl substituents.

Chemically Modulating Film Transport. Given the small pore size, we reasoned that binding molecules at appropriate sites within a membrane might serve to modulate the membrane's permeability. Porphyrin **5** features a coordinatively unsaturated zinc ion capable of axially binding aromatic nitrogen donors.[17] Transport of iodide through an unmodified film was observed in acetonitrile solution using tetrabutylammonium iodide with lithium perchlorate electrolyte. (Although the tetrabutylammonium cation cannot permeate the membrane, it was needed for solubility.) The film-modified electrode was placed in a 100 mM

solution of benzimidazole (**7**) for 5 min. The membrane-covered electrode was then returned to the iodide-containing solution. After one voltammetric cyclic (ca. 1 min), the current had been attenuated by a factor of 10. Successive scans over a period of about 20 min showed decreasing current to the point that only 1/100 of the original current was observed, and the film was essentially completely shut off with respect to iodide permeation (Figure 5).[18] Coordination of **7** was corroborated by a slight red shift in the Soret-region absorption maximum of the membrane (measurements with films on glass platforms). In retrospect, it is somewhat surprising that attenuation is so complete, given that porphyrin-coordinated Zn(II) ions bind only one ligand axially, not two. Finally, similar measurements with a smaller modifier, imidazole (**8**), revealed a roughly factor-of-2 decrease in iodide flux.
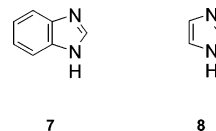
Conclusions

Nanoporous polymeric membranes can be formed by copolymerizing at a liquid/liquid interface a sterically demanding tetraphenylporphyrin derivative having reactive phenol substituents and a porphyrin having reactive acid chloride groups. The out-of-plane steric demand is created by 3,5-hexoxyphenyl groups positioned at two of the four meso carbons of the porphyrin ring. The bulky substituents create local pockets and extended pores within the resulting ester-linked copolymer. Quantitative measures of molecular and ionic transport can be obtained by placing membranes over microelectrodes and recording voltammetric responses from redox-active probes. From these measurements, the membranes were found to be permeable to small molecules and ions, but blocking toward larger ones, displaying a sharp size cutoff at a probe diameter of ca. 3.5 Å. Molecular transport can be attenuated by axially ligating imidazole to the Zn(II) center of the pocket-creating porphyrin. Transport can be essentially completely blocked by ligating benzimidazole.

(17) Bélanger, S.; Keefe, M. H.; Welch, J. L.; Hupp, J. T. *Coord. Chem. Rev.* **1999**, *190−192*, 29−45.

(18) Multiple attempts were made to remove the benzimidazole, including soaking the electrode-supported membrane in pure acetonitrile and in 10% perchloric acid. Neither approach removed the benzimidazole, and higher concentrations of acid dissolved the membrane. The persistence of ligand binding in the film environment, although difficult to explain, has been encountered previously; see ref 17.